Hydration Behavior of Alkyl Amines and Their Corresponding Protonated Forms. 1. Ammonia and Methylamine

Holger Hesske* and Karsten Gloe

TU Dresden, Department of Chemistry and Food Chemistry, 01062 Dresden, Germany

Received: April 24, 2007; In Final Form: July 20, 2007

The structure and dynamics of hydration of ammonia/ammonium and methylamine/methylammonium systems have been studied by Car−Parrinello molecular dynamics simulation. While methylamine interacts weakly with the aqueous environment, the interaction of ammonia is found to be much stronger than expected. Both protonated species show a highly structured first solvation sphere. The solvent exchange mechanisms for all species were also investigated, along with the geometry of the hydration spheres. Comparison of these exchange mechanisms with that published for the ammonium ion shows only a minor difference. Analysis of the respective distribution functions has allowed insight into the thermodynamics of solvation for both systems. The calculated pK_a values (9.23/10.65) correspond very closely with the published experimental values of 9.25 and 10.65.

I. Introduction

During the past decade the modeling of condensed phases has received a large amount of attention.[1−5] The development of computing power, new tools and methods as well as improved force-fields, higher basis sets, and more sophisticated functionals has made computational chemistry an important tool for researchers. An increasingly popular technique—the ab initio MD simulation procedure—has been developed to improve the investigation of condensed phases. In particular the Car−Parrinello approach,[6] based on density functional theory, showed high applicability to such systems.[1,7] The main advantage of the use of ab initio MD simulations when compared with time independent ab initio calculations with an empirical continuum solvent model is that the treatment of solute and solvent are handled on an equal footing without external parametrization. Nevertheless, the biggest problem in modeling fluid systems is to treat the influence of the solvent in a satisfactory manner. High level calculations are time- and resource-consuming, so that it is often necessary to reduce the solvation environment to small clusters; while empirical models, which more readily can handle large systems, often neglect electronic effects.

An area which relies on a detailed description of solvation is the hydration behavior of amines. The property of amines to act as an ambivalent receptor for either cations[8] or anions[9,10] depends strongly on their solvation and the pH-value. Especially the development of new separation processes for valuable or toxic species requires an extensive knowledge of these factors of influence.[11,12] Also the great importance of amines in biochemical reactions is mainly associated with their hydration and/or protonation behavior. It is commonly accepted that the irregular ordering of amine basicities is associated with solvation. An early work by Rao and Singh[13] has demonstrated that particular properties of the solvation of amines could be modeled by computational methods. In the 1990s several papers were published that dealt with different methods, parameters, or approaches in connection with amine hydration.[14−21] More recently, several new approaches and enhanced methods have been published that move toward a detailed and comprehensive description.[22−25] Even so, in such studies it has to be concluded that one or more parameters were generally described very well, while others deviated significantly from the corresponding experimental values. The goal of the present work was to attempt an exact and detailed description of amine hydration without using empirical parameters. In our approach both the amine itself and also its protonated form were included in the overall description.

II. Methods

A. Computational Details. All simulation systems contained 62 H_2O molecules and the relevant amine/ammonium ion. All hydrogen atoms were replaced by deuterium atoms to increase the time step. This change did not affect the structural properties of the system, only its motion and frequency, which were decreased by $\sqrt{2}$ to a first approximation, corresponding to the change in the moment of inertia. In the case of the ammonium and methylammonium ions one deuterium nucleus was removed from a randomly chosen water molecule to maintain charge neutrality in the box. Average distances between the OH^- generated and the nitrogen atoms were calculated to be 6.5 Å for all simulations. Furthermore, the distribution functions $g_{OO}(r)$ for the OH^- and the water oxygen atoms were calculated and compared with the results of Tuckerman et al.[26] The first peak of $g_{OO}(r)$ at 2.7 Å (calculated by Tuckerman et al.) was reproduced well in this work. The first minimum at 3.5 Å was found to be 0.5, which is significantly higher than the literature value. Nevertheless, the distribution functions were nearly 1 at greater distances (>4.5 Å). Reflecting this, the thermodynamic and dynamic properties of the first shell surrounding the amines are not expected to be affected by the presence of the hydroxide ion.

A cubic supercell with a cell length of $a = 12.4$ Å was chosen for the simulations, and periodic boundary conditions were applied. To investigate whether the results were size-consistent, classical MD runs were performed with the 4-fold axis length

* To whom correspondence should be addressed. E-mail: holger.hesske@chemie.tu-dresden.de.

10.1021/jp073154a CCC: $37.00
Published on Web 09/06/2007

of the simulation box.[27] The simulations showed that the estimated second hydration sphere was fully described within the simulation box, which is consistent with other reports.[28,29] All simulations were performed using the CPMD package,[30] starting from an equilibrated classical MD run. Using the Car−Parrinello approach, the equations of motion were integrated with a fictious electron mass of 600 au and a time step of 0.121 fs. All data were averaged from a microcanonical ensemble (NVE) over a production run of 10 ps at 300 K. The gradient corrected BLYP exchange-correlation functional was used to compute the electronic structure within the Kohn−Sham formulation, and a cutoff radius of 70 Ry was employed.[31,32] Although the use of the BLYP functional leads to strong decreased self-diffusion,[2] it has been shown to provide a reasonable description of the properties of aqueous systems.[28] Pseudopotentials in Troullier−Martins form,[33] which are present in the CPMD program were transformed into the fully nonlocal form by the Kleinman−Bylander separation procedure.[34] Similar approaches have been published and show good agreement with experimental results.[26,35−38]

B. Calculation of pK_a from the Distribution Functions. A definition of the equilibrium constant K_a for a protonation reaction is given from the law of mass action:

$$AH^+ \rightleftharpoons A + H^+$$

$$K_a = \frac{[A][H^+]}{[AH^+]} \quad (1)$$

From a statistical view eq 1 can be described as the relation of probabilities, where the proton either belongs to the donor atom or does not. If the concentration inside a simulation box of volume V is c_0 and $P(R_C)$ is the probability of finding a proton within a radius R_C from the donor atom, K_a can be expressed by

$$K_a = \frac{(1 - P(R_C))^2}{P(R_C)c_0V} \quad (2)$$

It is obvious that the choice of R_C crucially influences the estimated K_A values. The value 1.12 Å used for R_C was calculated from water−ammonium clusters based on density functional theory with the B3LYP functional and the 6-311+G* basis set. The free energy of the clusters was calculated using stepwise elongation of one N−H bond and show a gradient maximum at R_C. Similar approaches have been published for the self-ionization of water[39] and the deprotonation of $P(OH)_5$.[40]

III. Results and Discussion

A. Ammonia/Ammonium. Inspired by the work of Bruge et al.,[28] who described the rotational dynamics of the ammonium ion by CPMD, we were led to undertake the simulation of the ammonia/ammonium ion system as a first goal of the present work. A trajectory for the ammonium ion was again calculated, and the results were almost identical to those obtained by the above authors. The differences in the pair correlation functions g(NO) (Figure 1) beyond the first minimum were mainly a result of the lower fictitious mass employed. During the simulation of the ammonia system spontaneous protonation events were observed, and these results were excluded from further analyses. In general, a set of pair correlation functions (pair distribution functions) were successful in describing a solvated system completely. Comparisons of the resulting oxygen−oxygen distribution and the water hydrogen-oxygen distribution with

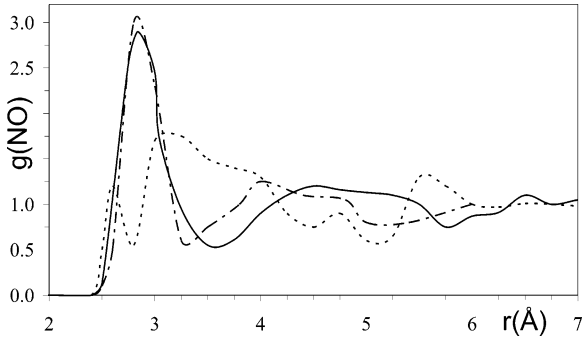

Figure 1. Partial distribution functions g(NO) calculated from 10 ps microcanonical production runs and smoothed about 0.2 Å by performing a running average using ten points. Results for ammonium were represented by solid (this work) and dashed-dotted line (Bruge et al.[28]). The dashed line represents the results for ammonia (this work).

TABLE 1: Averaged Hydrogen Bond Lengths [Å]

	simulation average		X-ray data[41]	
donors	N−H···O	N···O	N−H···O	N···O
NH_4^+	1.93	2.94	1.95(1)	2.91(1)
CH_3-NH_2		3.02	2.016(6)	2.963(5)
CH_3-NH_3^+	2.02	2.82	1.878(6)	2.963(5)
acceptors	N···H−O	N···O	N···H−O	N···O
NH_3	1.74	2.68		
CH_3-NH_2	1.78	2.74	1.88	2.84

those obtained by Todorova et al.[2] or van Erp et al.[29] confirm that the chosen simulation conditions led to good agreement with the prior results.

The distribution functions were generated from the trajectory configurations taken every 20 fs, which is slightly longer than the reorganization time of hydrogen bonds in water. For the systems investigated the g(NO) function is of crucial importance for gaining a deep insight into the amine solvation. As shown in Figure 1, the difference between the different species is very great. For the ammonium ion a clear first hydration sphere was observed for g(NO) with a maximum of 2.9 at a distance of 2.8 Å. Integration up to the first minimum at 3.5 Å led to a coordination number of around 5.4, which shows general consistency with the published results of Bruge et al.[28] The slightly less structured distribution might be due to a smaller fictitious mass[42] used in this work. A completely different picture was observed for ammonia. The nearest peak at 2.6 Å is related to the N···H−O hydrogen bond, where the nitrogen atom acts as electron pair donor. A much broader plateau (2.8−4.5 Å) is related to two different kinds of water molecules. The water molecules, which interact weakly with the amine hydrogen atoms, were placed at a distance of 2.8−3.3 Å, while those placed between 3.2 and 4.5 Å were noninteracting with the amine but interacted with a strongly bonded water molecule in the first hydration sphere. The hydrogen bonds, analyzed and averaged over all configurations, were compared with published bond lengths from crystal structures[41] and were in good agreement (Table 1). As expected ammonia has a less structured first hydration sphere and the interactions between the solvent molecules seemed to be more geometry determined. Surprisingly the coordination number calculated up to a distance of 3.5 Å is 7.2. This means that, on average, the ammonia molecule is surrounded by two more water molecules than the ammonium ion. These results were analyzed more precisely by aligning all configurations of the trajectories to an N−H bond (ammonium ion), or to the vector of the free electron pair (ammonia), respectively. This alignment allowed a calculation of a density

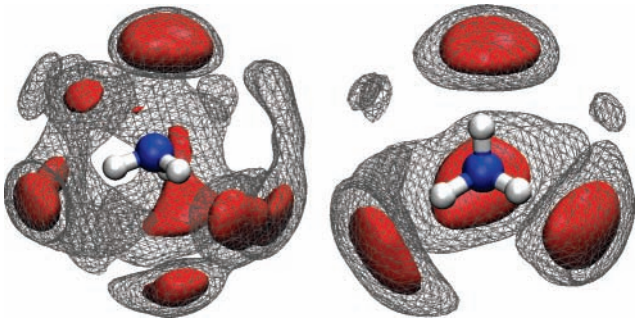

Figure 2. Spatial distribution maps created with the VMD-software[43] for the first hydration spheres of ammonia (left) and ammonium (right). The isosurfaces were obtained from the average of all configurations and represent 92% (red) and 97% (wireframe) of the oxygen density.

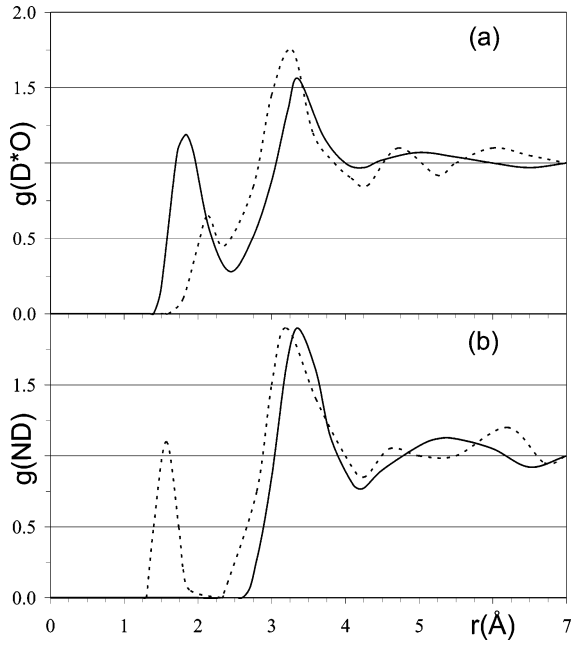

Figure 3. Partial distribution functions **(a)** g(ND) (D denotes water hydrogen) and **(b)** g(D*O) (D* denotes amine hydrogen) calculated from 10 ps microcanonical production runs and smoothed about 0.2 Å by performing a running average using ten points. Solid and dashed line represent ammonium and ammonia, respectively.

map (Figure 2) for the oxygen atoms surrounding the amine. In agreement with the literature,[28] the displayed isosurfaces of oxygen density depict that in the case of ammonium a stable cage of four water molecules is formed. Another water molecule was found to enter the first hydration sphere in several positions. The results for ammonia represent more delocalized hydrogen-bonded water molecules and also additional water molecules in the first hydration sphere, which are not hydrogen bonded to ammonia. Figure 3 depicts the distribution functions *g*(ND) and *g*(D*O), which also show some interesting features. Integration of *g*(D*O) up to the first minimum yielded to the coordination numbers for the ammonia/ammonium hydrogen atoms. While all ammonium hydrogen atoms are on average coordinated by one water molecule, ammonia hydrogen atoms are only coordinated by 0.7 water molecules. This result indicates also that the first hydration sphere of ammonia is highly mobile. In addition the nitrogen−water hydrogen distributions *g*(ND) (Figure 3b) show some differences between ammonia and ammonium. The additional peak at 1.6 Å represents the hydrogen bond involving the lone pair of the nitrogen. The peaks for ammonium are shifted about 0.25 A away from the nitrogen relative to those of ammonia.

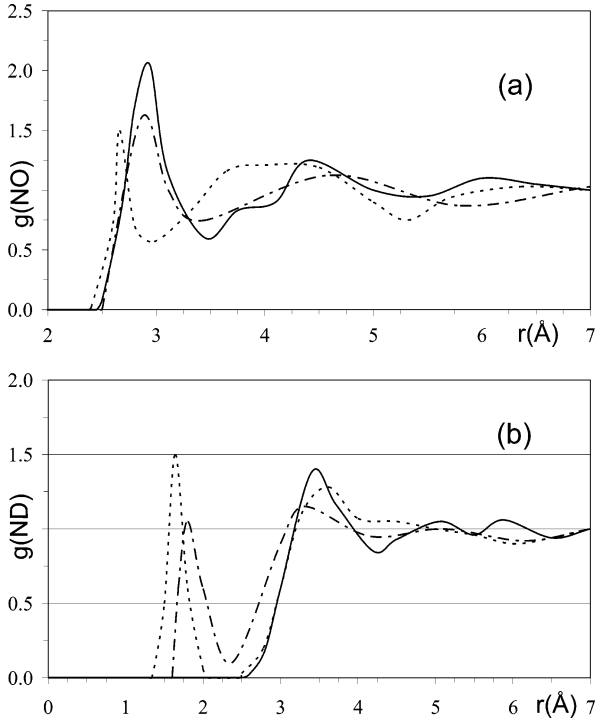

Figure 4. Partial distribution functions (a) *g*(NO) and (b) *g*(ND) (D denotes water hydrogen) calculated from 10 ps microcanonical production runs and smoothed about 0.2 Å by performing a running average using 10 points. Solid and dashed lines represent methylammonium and methylamine, respectively. The dashed dotted lines represent results from Kusalik et al.[22]

B. Methylamine/Methylammonium. *1. Radial Distributions.* In a difference to the ammonium ion, neither methylamine nor ammonium have been investigated by CPMD so far. As observed for ammonia, some production runs of methylamine showed a proton transfer from water to the amine, leading to an associated ion pair. These results were excluded from the calculation of the distribution functions and also in further analyses.

The partial distribution functions *g*(NO) and *g*(ND) are displayed in Figure 4. The *g*(NO) function for methylammonium showed a similar trend to that of ammonium. While a distinct first hydration sphere between 2.4 and 3.5 Å exists for the protonated species, a second hydration sphere is hardly evident. The observed small shoulder for methylammonium at 3.75 Å belongs to the second hydration sphere but is fused with a peak assigned to water molecules nearest to carbon. The nitrogen-oxygen distribution for methylamine is characterized by a small peak at 2.65 Å, which can be assigned to a water molecule interacting strongly with the nitrogen lone pair. The distribution between 3.0 and 5.3 Å is caused by different types of water molecules. Amine-interacting water molecules were assigned between 3.0 and 3.8 Å, while water molecules between 3.6 and 5.3 Å corresponded to a second hydration sphere. A comparison of *g*(ND) (Figure 4b) showed only slight differences between the calculations for the respective species. The additional peak for methylamine at 1.7 Å was assigned to the deuterium atom of the nearest coordinated water molecule, while the differences between 3.2 and 4.6 Å are within statistical uncertainty.

Closer examination of the distribution functions with respect to the protonation state, revealed some unexpected behavior. Due to protonation the peak maximum shifted from 2.65 to 3.0 Å and rose from 1.5 to 2.1 for the nitrogen−oxygen distribution. While the observed higher maximum (caused by additional electrostatic interactions) was expected, the fact that the

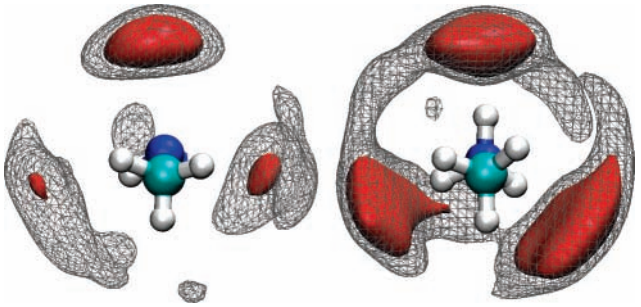

Figure 5. Spatial distribution maps created with the VMD-software[43] for the first hydration spheres of methylamine (left) and methylammonium (right). The isosurfaces were obtained from the average of all configurations and represent 94% (red) and 97% (wireframe) of the oxygen density.

maximum occurred at a greater distance can only be explained by steric interactions occurring between the water molecules inside the first hydration sphere.

Methylamine was thoroughly studied by Kusalik et al.[22] using a different method. These authors obtained distribution functions which are also displayed in Figure 4. Surprisingly the *g*(NO) distribution for methylamine obtained by Kusalik et al. is similar to the *g*(NO) function of methylammonium obtained in this work. The peak maximum for the first hydration sphere of these g(NO) functions differed by 0.5, but as shown by Kusalik et al.[22] this can be a consequence of the concentration of methylamine in the solution.

2. Spatial Distributions. As shown by Kusalik et al.[22] investigation of the spatial distribution of the water molecules around the amine led to further insight into the nature of the hydration.

All configurations of methylamine/ammonium were aligned along the carbon-nitrogen and a ND* axis. An oxygen density map was calculated (Figure 5) for these aligned configurations and this aided a better understanding of the spatial distribution around the amine functionality. For the unprotonated amine it was found that only one water molecule was strongly hydrogen bonded (with an O−H···N bond), while both amine hydrogen atoms were only involved in weak hydrogen bonds. Reflecting the presence of these weak hydrogen bonds, the geometry of the amine environment is determined by the water−water interactions. A density map around the amine functionality within a distance of 3.5 Å showed a less structured distribution of the oxygen atoms compared with the map for ammonia. The solid isosurface was calculated for 94% of oxygen density (Figure 5), because 92% density (as used for ammonia (Figure 2)) led to an almost completely filled space around the amine. Although the first minimum of the *g*(NO) function for methylamine was found at 3.0 Å, the first hydration sphere includes hydrogen-bonded water molecules at a distance of 3.45 Å. Integration up to this radius led to a coordination number of 3.0 for methylamine.

In stark contrast to these results, the calculation for $CH_3NH_3^+$ showed a much more structured first hydration sphere (Figure 5). The oxygen atoms were localized in the directions of the ND* bonds, forming three strong hydrogen bonds. The bond lengths of these hydrogen bonds are slightly larger than those found for CH_3NH_2. Integration as above led to a coordination number of 4.2 at the first minimum. This means that an additional water molecule is present in the first hydration sphere and it is without a discrete position. This result is in good agreement with the results from the calculations for ammonia and the ammonium ion: While the protonated species show a highly structured first hydration sphere, with additional weakly bonded water molecules, the unprotonated species each show only one strong interaction.

TABLE 2: Calculated Coordination Numbers and Residence Times

species	coordination number	1st hydrogen sphere radius [Å]	residence times τ [ps] major (minor)
NH_3	7.2	3.5	1.2 (0.03)
NH_4^+	5.4	3.5	4.0 (0.08)[a]
CH_3NH_2	3.0	3.45	1.5 (0.05)
$CH_3NH_3^+$	4.2	3.45	2.7 (0.12)

[a] Taken from ref 28.

C. Coordination Numbers and Residence Times. As described by Bruge et al.,[28] a stable cage of water molecules was proposed to surround the ammonium ion, with an additional water molecule entering the first hydration sphere in various places. A similar (but not identical) behavior was proposed for $CH_3NH_3^+$ in this study. In contrast to the results obtained by the above authors, in the present study it was found that the additional water entered the first hydration sphere between two of the hydrogen-bonded water molecules and not in the plane between all three. For the unprotonated species the water molecules were found to exchange faster when weakly bonded via N−H···O bonds, while exchange for the N···H−O bond was not observed within the simulation time employed.

To confirm these results, a residence time according to the definition of Impey et al.,[44] based on the average coordination number $n(t)$, was calculated:

$$n(t) = \frac{1}{N}\sum_{n=1}^{N}\sum_{j} P_j(t_n, t) \qquad (3)$$

The coordination number was obtained from N atomic configurations and all j water molecules of the system. $P_j(t_n, t)$ was defined to be 1, if the water molecule was placed in the hydration sphere at time t_n and $t_n + t$, otherwise it is defined to be zero. At longer times, $n(t)$ decays exponentially as $e^{-t/\tau}$, where τ is by definition the residence time. The major residence time was assigned to the hydrogen-bonded water molecules, while the minor one was assigned to water molecules entering and leaving the first hydration sphere without being hydrogen bonded. The calculation of the coordination number and the residence time for the different species using this algorithm leads to the results displayed in Table 2.

The nonexchanged water molecules for the unprotonated species were omitted in the calculations because no exchange corresponds to infinite residence times. Both protonated molecules show a much higher major residence time, which is in accord with a stable cage of water molecules surrounding the protonated amine and additional water molecules entering this sphere from time to time. It needs to be mentioned, those residence times of 4.0/2.7 ps are less reliable when obtained by averaging over a simulation time of 10 ps. Also, because BLYP is now known to underestimate the self-diffusion coefficient of pure liquid water,[45] the calculated residence times might be overestimated. Nevertheless, the values show the existence of two kinds of mobility for the molecules within the hydration spheres. For the nonprotonated amines the major residence times are much smaller and the minor ones can be neglected because they are of a similar time scale to the reorganization times for hydrogen bonds in water (18 fs).

D. Exchange Mechanisms and pK_a Values. The exchange and the rotational mechanism were investigated in more depth to obtain more detailed insight into the above results. Com-

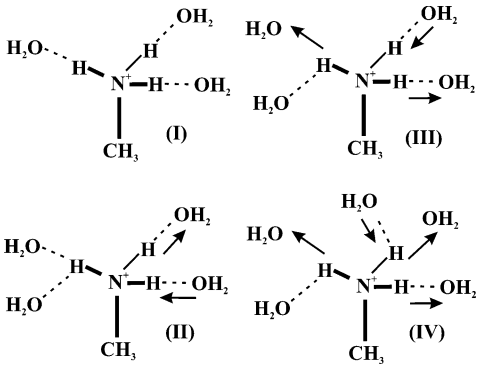

Figure 6. Calculated solvent exchange mechanism for $CH_3NH_3^+$.

TABLE 3: Calculated Probabilities of Deprotonation $P(R_C)$ and pK_a Values

species	$P(R_C)$	pK_a
NH_4^+	$5.56 \times 10^{-10} \pm 1 \times 10^{-12}$	9.23 ± 0.008
$CH_3NH_3^+$	$2.42 \times 10^{-11} \pm 1.6 \times 10^{-12}$	10.65 ± 0.016

parison with the results of Bruge et al.[28] shows a different solvent exchange for the methyl substituted ammonium ion. Reflecting the smaller residence time, about nine exchange events of the directly bonded water molecules were observed. Many additional events involving partial removal and re-entry of water molecules were also observed in all simulations. Eight of the nine observed exchanges can be described by the rotational mechanism outlined in Figure 6.

Initially three almost identical hydrogen bonds exist (I), but after a new water molecule enters the first hydration sphere, the hydrogen bonds begin to differ (II). One hydrogen bond becomes very strong ($\approx$2.75 Å, $\varphi(N^+-H\cdots O) = 180° \pm 5°$), while the hydrogen bond next to the new water molecule become quite weak ($\approx$3.2 Å, $\varphi(N^+-H\cdots O) = 140° \pm 20°$). This might be caused by steric effects between the water molecules. The third water molecule forms a bifurcated structure involving the new solvent molecule. The original water molecule is removed from the first hydration sphere in about 100−180 fs, while the new one forms a moderately strong hydrogen bond. From this point several pathways become possible. One involves the re-stabilizing of the original hydrogen bonds (III), while another gives rise to an additional exchange at the weakly bonded side (IV). This additional exchange is calculated to be comparatively fast (50−80 fs).

For ammonia and methylamine several exchange events were observed, but no detailed exchange mechanism was elucidated. In some cases the weakly bonded water molecules were exchanged via a bifurcated structure with the new water molecule. While in other cases the water molecule left the first hydration sphere and subsequently a new one entered and formed a hydrogen bond.

As noted above the probabilities of deprotonation $P(R_C)$ were calculated for the protonated species from all configurations and all simulations. For the ammonium ion more than 15 000 configurations were analyzed, while for the methylammonium about 10 000 configurations were involved. As shown in Table 3 the probabilities were calculated with high precision and led to pK_a values which agree very well with the experimental ones.[46,47] While the chosen R_C led to exact results, it is still necessary to probe whether a similar choice is applicable to related molecules.

IV. Conclusions

In this study the solvation of ammonia/ammonium ion and methylamine/methylammonium ion by DFT based molecular dynamics simulation (CPMD) was investigated. The BLYP functional used has been shown to reproduce the structures of similar systems studied in good agreement with experimental results.[2,28]

It was shown that the hydration spheres adjacent to the amine or ammonium nitrogen atoms differ significantly. This is apparent from the radial distribution functions and, in a more detailed way, by the spatial distribution function for the water oxygen around the nitrogen atoms. More precisely, the radial distribution shows that the solvation structure of the different species is identical beyond the first hydration shell, while inside the hydration sphere the structure is quite different. The unprotonated species show a similar behavior, with the lone pair of each nitrogen strongly interacting with a water molecule. The amine hydrogen atoms form only weak hydrogen bonds with water, which undergoes comparably fast exchange. The protonated species gives rise to a stable cage of water molecules via formation of strong hydrogen bonds. The exchange of these water molecules is rather slow, as shown by the calculated residence times. Estimated coordination numbers show that ammonia is on average coordinated by more water molecules than ammonium, while in the case of methylamine the protonated form has a higher coordination number. Furthermore, the protonation constants were calculated from all data with high precision and in good agreement with the experimental values.[46] Finally, it is noted that the present results have implications for the prediction of the basicity of alkyl amines in aqueous solution.

Acknowledgment. This work was supported by the DFG (Deutsche Forschungsgemeinschaft). The authors also acknowledge the ZIH (Zentrum für Hochleistungsrechnen) of the TU Dresden for the use of the supercomputer facilities and George Wipff, Strasbourg for helpful discussions.

References and Notes

(1) Carloni, P.; Rothlisberger, U.; Parrinello, M. *Acc. Chem. Res.* **2002**, *35*, 455−464.
(2) Todorova, T.; Seitsonen, A. P.; Hutter, J.; Kuo, F. W.; Mundy, C. J. *J. Phys. Chem. B* **2006**, *110*, 3685−3691.
(3) Freedman, H.; Truong, T. N. *J. Chem. Phys.* **2004**, *121*, 2187−2198.
(4) Bagchi, B. *Annu. Rep. Prog. Chem. C* **2003**, *99*, 127−175.
(5) Jorgensen, W. L.; Tirado-Rives, J. *Proc. Natl. Acad. Sci. U.S.A.* **2005**, *102*, 6665−6670.
(6) Car, R.; Parrinello, M. *Phys. Rev. Lett.* **1985**, *55* (22), 2471−2474.
(7) Iftimie, R.; Minary, P.; Tuckerman, M. E. *Proc. Natl. Acad. Sci. U.S.A.* **2005**, *102*, 6654−6659.
(8) Bianchi, A.; Micheloni, M.; Paoletti, P. *Coord. Chem. Rev.* **1991**, *110*, 17−113.
(9) Wichmann, K.; Antonioli, B.; Söhnel, T.; Wenzel, M.; Gloe, K.; Gloe, K.; Price, J. R.; Lindoy, L. F.; Blake, A. J.; Schröder, M. *Coord. Chem. Rev.* **2006**, *250*, 2987−3003.
(10) Bianchi, A., Bowman-James, K., Garcia-Espana, E., Eds. *Supramolecular Chemistry of Anions*; Wiley-VCH: New York, 1997.
(11) Stephan, H.; Juran, S.; Antonioli, B.; Gloe, K.; Gloe, K. In *Analytical Methods in Supramolecular Chemistry;* Schalley, C., Ed.; Wiley-VCH: Weinheim, Germany, 2006.
(12) Gloe, K.; Antonioli, B.; Gloe, K.; Lindoy, L. In *Encyclopedia of Supramolecular Chemistry;* Atwood, J. L., Steed, J. W., Eds.; Marcel Dekker: New York, online, 2006.
(13) Rao, B. G.; Singh, U. C. J. *J. Am. Chem. Soc.* **1989**, *111*, 3125−3133.
(14) Wan, S.; Stote, R. H.; Karplus, M. *J. Chem. Phys.* **2004**, *121*, 9539−9548.
(15) Rizzo, R. C.; Jorgensen, W. L. *J. Am. Chem. Soc.* **1999**, *121*, 4827−4836.
(16) Morgantini, P. Y.; Kollman, P. A. *J. Am. Chem. Soc.* **1995**, *117*, 6057−6063.
(17) Ding, Y. B.; Bernardo, D. N.; Krogh-Jespersen, K.; Levy, R. M. J. *J. Phys. Chem.* **1995**, *99*, 11575−11583.
(18) Meng, E. C.; Caldwell, J. W.; Kollman, P. A. J. *J. Phys. Chem.* **1996**, *100*, 2367−2371.

(19) Marten, B.; Kim, K.; Cortis, C.; Friesner, R. A.; Murphy, R. B.; Ringnalda, M. N.; Sitko, D.; Honig, B. *J. Phys. Chem.* **1996**, *100*, 11775−11788.
(20) Cramer, C. J.; Truhlar, D. G. J. *J. Comput.-Aided Mol. Des.* **1992**, *6*, 629−666.
(21) Kawata, M.; Tenno, S.; Kato, S.; Hirata, F. *J. Am. Chem. Soc.* **1995**, *117*, 1638−1640.
(22) Kusalik, P. G.; Bergman, D.; Laaksonen, A. *J. Chem. Phys.* **2000**, *113*, 8036−8046.
(23) Liu, D.; Wyttenbach, T.; Bowers, M. *Int. J. Mass Spectrom.* **2004**, *236*, 81−90.
(24) Hofer, T. S.; Tran, H. T.; Schwenk, C. F.; Rode, B. M. *J. Comput. Chem.* **2004**, *25*, 211−217.
(25) Oostenbrink, C.; Juchli, D.; van Gunsteren, W. F. *Chem. Phys. Chem.* **2005**, *6*, 1800−1804.
(26) Tuckerman, M.; Laasonen, K.; Sprik, M.; Parrinello, M. *J. Chem. Phys.* **1995**, *103*, 150−161.
(27) *Materials Explorer*, 2nd ed.; Fujitsu Limited: Sunnyvale, CA, 2000.
(28) Brugé, F.; Bernasconi, M.; Parrinello, M. *J. Am. Chem. Soc.* **1999**, *121*, 10883−10888.
(29) van Erp, T. S.; Meijer, E. J. *J. Chem. Phys.* **2003**, *118*, 108831−8840.
(30) *CPMD*, version 3.7.2; IBM Corp.: Armonk, NY, 1990−2002.
(31) Becke, A. D. *Phys. Rev. A* **1988**, *38*, 3098−3100.
(32) Lee, C.; Yang, W.; Parr, R. G. *Phys. Rev. B* **1988**, *37*, 785−789.
(33) Troullier, N.; Martins, J. L. *Phys. Rev. B* **1991**, *43*, 1993−2006.
(34) Bylander, D. M.; Kleinmann, L. *Phys. Rev. B* **1990**, *41*, 907−912.
(35) Tobias, D. J.; Jungwirth, P.; Parrinello, M. *J. Chem. Phys.* **2001**, *114*, 7036−7044.
(36) Kreitmeir, M.; Bertagnoli, H.; Mortensen, J. J.; Parrinello, M. *J. Chem. Phys.* **2003**, *118*, 3629−3645.
(37) Ramaniah, L. M.; Bernasconi, M.; Parrinello, M. *J. Chem. Phys.* **1999**, *111*, 1587−1591.
(38) Ramaniah, L. M.; Bernasconi, M.; Parrinello, M. *J. Chem. Phys.* **1998**, *109*, 6839−6843.
(39) Davies, J. E.; Doltsinis, N. L.; Kirby, A. J.; Roussev, C. D.; Sprik, M. *J. Am. Chem. Soc.* **2002**, *124*, 6594−6600.
(40) Doltsinis, N. L.; Sprik, M. *Phys. Chem. Chem. Phys.* **2003**, *5*, 2612−2618.
(41) Steiner, T. *Angew. Chem.* **2002**, *114*, 50−80.
(42) Grossman, J. C.; Schwegler, E.; Draeger, E. W.; Gygi, F.; Galli, G. *J. Chem. Phys.* **2004**, *120* (1), 300−311.
(43) Humphrey, W.; Dalke, A.; Schulten, K. *J. Mol. Graph.* **1996**, *14*, 33−38.
(44) Impey, R. W.; Madden, P. A.; McDonald, I. *J. Phys. Chem.* **1983**, *87*, 5071−5083.
(45) VandeVondele, J.; Mohamed, F.; Krack, M.; Hutter, J.; Sprik, M.; Parrinello, M. *J. Chem. Phys.* **2005**, *122*, 014515.
(46) Kilic, E.; Gokce, G.; Canel, E. *Turk. J. Chem.* **2002**, *26*, 843−849.
(47) Ben-Naim, A.; Marcus, Y. *J. Chem. Phys.* **1984**, *81*, 2016−2027.